Facies (2012) 58:261–278
DOI 10.1007/s10347-011-0278-9

ORIGINAL ARTICLE

Stable isotope analyses of belemnites from the Kachchh Basin, western India: paleoclimatic implications for the Middle to Late Jurassic transition

Matthias Alberti · Franz T. Fürsich · Dhirendra K. Pandey · Mu. Ramkumar

Received: 20 December 2010 / Accepted: 17 October 2011 / Published online: 5 November 2011

Abstract Stable isotope analyses of 61 diagenetically unaltered belemnite rostra from the Middle to Late Jurassic of the Kachchh Basin of western India suggest stable paleotemperatures across the Callovian-Oxfordian boundary (~14°C). Only at the end of the Middle Oxfordian water temperatures drop for more than 3°C before reaching again higher values during the Kimmeridgian (~12.3°C). The data do not support polar glaciations proposed for the Middle to Late Jurassic transition, which necessarily would have led to a global temperature and sea-level minimum at the boundary. Callovian to Oxfordian rocks in the Kachchh Basin point to a gradual shallowing corresponding to a slight fall in relative sea level. However, the magnitude of this regression is comparatively small, and the sea-level minimum is reached in the late Early Oxfordian and not close to the boundary. Results from the Kachchh Basin therefore, imply almost stable climatic conditions during the Middle to Late Jurassic transition and do not show any evidence for polar glaciations.

Keywords Oxygen and carbon isotopes · Paleoclimate · Jurassic · Kachchh Basin · India

M. Alberti (✉) · F. T. Fürsich
GeoZentrum Nordbayern, Fachgruppe PaläoUmwelt, Friedrich-Alexander-Universität Erlangen-Nürnberg, Loewenichstraße 28, 91054 Erlangen, Germany
e-mail: matthias.alberti@gzn.uni-erlangen.de

D. K. Pandey
Department of Geology, University of Rajasthan, Jaipur, 302004, India

Mu. Ramkumar
Department of Geology, Periyar University, Salem 636011, India

Introduction

The Jurassic rocks of the Kachchh Basin have been studied for over a century beginning with studies by Grant (1840) and Wynne (1872). Since then the area has become increasingly important as a key area for the Gondwanian margin of the Neotethys. Studies on the evolution of the Kachchh Basin allow inferences on the development of the Malagasy Gulf, the Arabian Sea, and the incipient western Indian Ocean.

The Middle to Late Jurassic transition aroused interest after Dromart et al. (2003a, b) suggested a glacial phase connected with a global sea-level fall during this time span. These authors combined results of stable isotope analyses with sedimentary and faunal evidence in support of their hypothesis. Their assumption contradicts earlier opinions, according to which the Callovian–Oxfordian boundary is a time of sea-level high stand (Norris and Hallam 1995; Hallam 2001). Hallam (2001) suggested that for the whole Jurassic period there is no evidence for waxing and waning polar icecaps and that it is highly unlikely that there was ever sufficient ice to produce larger sea-level changes. Most recently, Wierzbowski et al. (2009) proposed a global sea-level rise for the Late Callovian thereby reinterpreting arguments given by Dromart et al. (2003a, b).

The purpose of the present study is to shed further light on the paleoclimatic conditions around the Middle to Late Jurassic transition by analysing stable oxygen isotopes of belemnite rostra from this interval. The rocks of the Kachchh Basin, which so far have only cursorily been studied from this point of view (Fürsich et al. 2005), are particularly well suited for this purpose, because of their wide distribution and a number of associated sedimentary and diagenetic features, which provide inferences about the relative sea-level fluctuations.

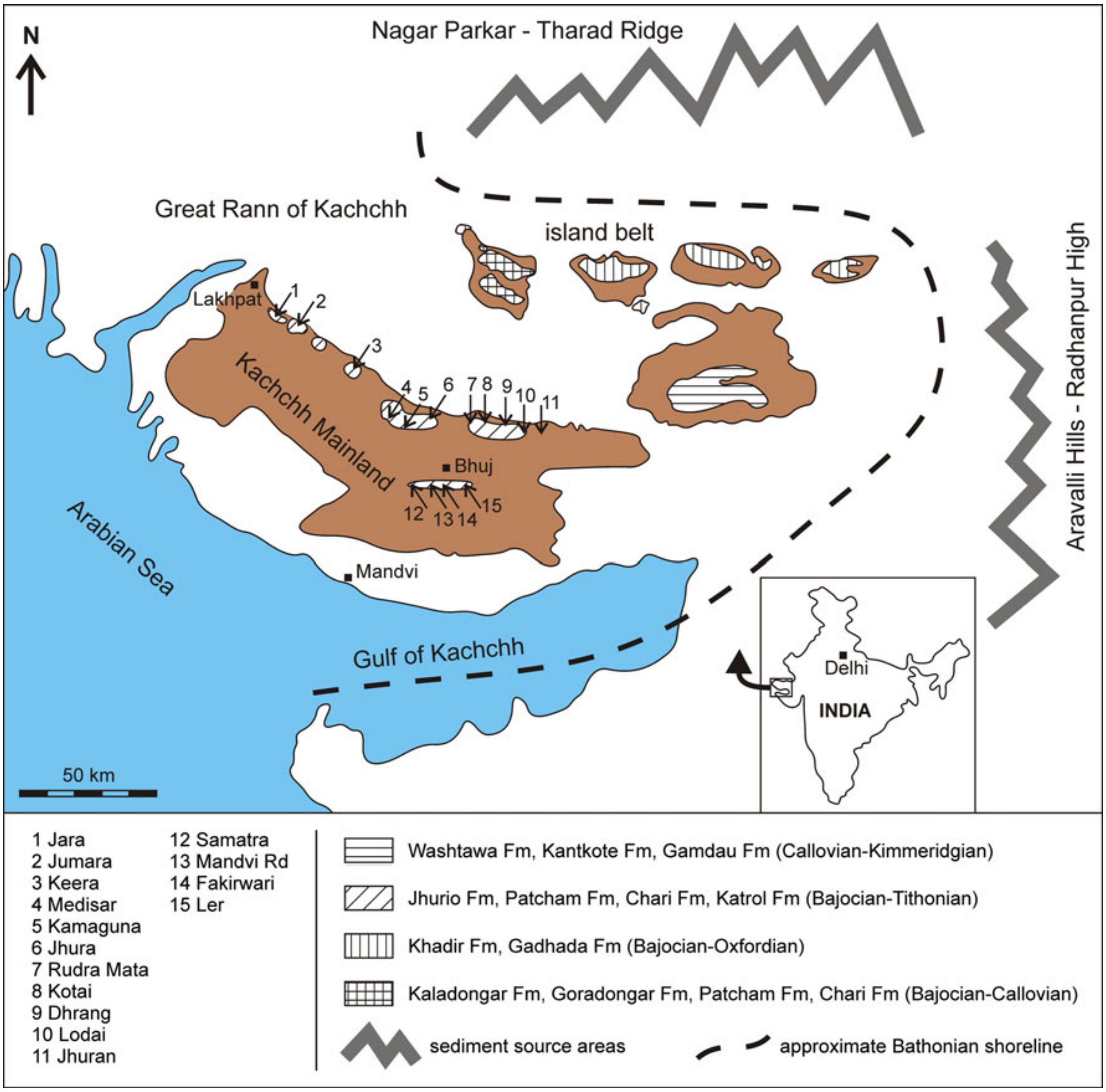

Fig. 1 Geological sketch map of the Kachchh Basin showing the location of the studied sections on Kachchh Mainland (modified after Fürsich et al. 2004a, 2005)

Geological and paleogeographical setting

The Kachchh Basin, situated at the western margin of the Indian craton (Fig. 1), formed following rifting between Africa and India in the Late Triassic (Biswas 1982, 1991). After an initial phase of terrestrial sedimentation in the Late Triassic and Early Jurassic, the sea of the Malagasy Gulf inundated the basin in the Bajocian or even earlier (Singh et al. 1982; Fürsich 1998; Fürsich et al. 2001, 2004a). Since then marine conditions dominated in the small basin at the eastern margin of this narrow southerly extension of the Tethys (Fig. 2) until it was filled with siliciclastic sediments in the early Cretaceous. The studied sections comprise sediments of Late Callovian to Kimmeridgian age. During this time, the paleolatitude of the Kachchh Basin did not change considerably and was presumed to be between 25° S (Smith et al. 1994) and 30° S (Riccardi 1991).

Jurassic outcrops of the Kachchh Basin have generally been divided into two groups, an E-W oriented chain of domal structures on Kachchh Mainland between the salt marshes of the Great Rann of Kachchh to the north and the Arabian Sea to the south and an island belt to the north and east of the mainland. The domes on Kachchh Mainland offer outcrops from Bajocian to Tithonian in age (Fürsich et al. 2004a, b; Krishna et al. 2009a). Sediments of the island belt are mainly somewhat older.

The litho- and biostratigraphic framework for the studied sections of Kachchh Mainland is given in Fig. 3. Deposition of fine-grained siliciclastics of the Chari Formation started during the Callovian. The sections begin

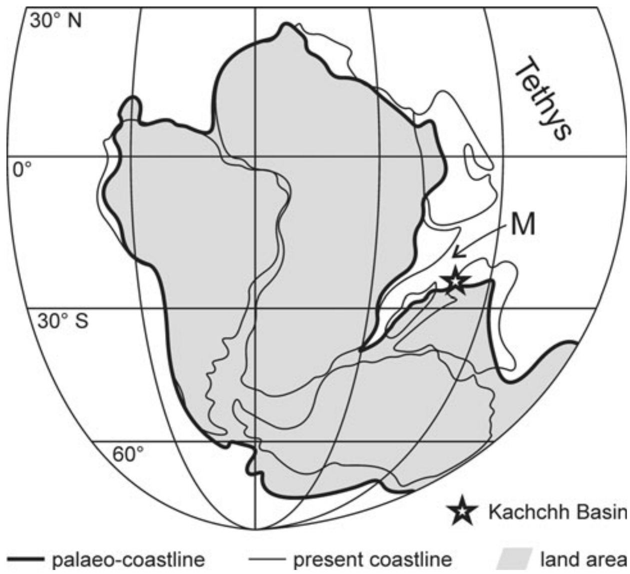

Fig. 2 Paleogeographical setting of the Kachchh Basin during the Middle to Late Jurassic transition (modified after Smith et al. 1994). *M* Malagasy Gulf

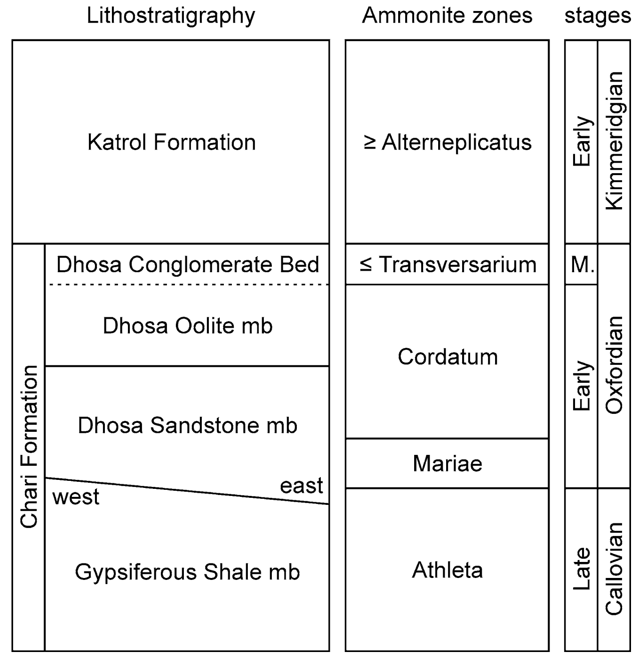

Fig. 3 Litho- and biostratigraphic framework across the Middle to Late Jurassic transition on Kachchh Mainland (modified after Krishna et al. 1996a; Alberti et al. 2011; John H. Callomon pers. comm. 2000)

within the Upper Callovian Gypsiferous Shale member, which is dominated by bioturbated argillaceous silt. The sediment contains several levels of small concretions and abundant secondary gypsum. While crossing the Middle to Late Jurassic boundary the Gypsiferous Shale member is coarsening-upwards into the Dhosa Sandstone member, which comprises beds of fine-grained sandstone. The sediment is bioturbated and occasionally cross-bedded indicating a slightly higher energy level caused by a lower relative sea level. Following on top of the Dhosa Sandstone is the Dhosa Oolite member, whose name derives from allochthonous, ferruginous ooids, which occur scattered and in varying abundance in the sediment. This unit has received considerable attention (e.g., Singh 1989; Fürsich et al. 1992) due to its highly complex top unit, the Dhosa Conglomerate Bed. This marker bed, which can be traced throughout Kachchh Mainland for over 100 km, is highly condensed and contains abundant, though mostly reworked, ammonites. In a few sections another zone of fine siltstone follows on top of the Dhosa Conglomerate Bed. The stratigraphic affiliation of this unit is still not clear; partly it shows a strong resemblance to the Dhosa Oolite member, but has not yet yielded any ammonites for biostratigraphic correlation. Finally, after a depositional gap, coarse sandstones of the Katrol Formation follow.

Biostratigraphy

The biostratigraphy of the Jurassic sediments of the Kachchh Basin is strongly based on ammonites, which have been studied for more than 100 years. Biostratigraphic studies in the region started with the fundamental monographs on cephalopods by Waagen (1873–1875) and Spath (1927–1933) and continue until today (e.g., Bardhan et al. 1979, 1988; Singh et al. 1982, 1983; Jaitly and Singh 1983; Pandey and Agrawal 1984; Agrawal and Pandey 1985; Bardhan and Datta 1987; Krishna and Westermann 1987; Pandey and Westermann 1988; Pandey et al. 1994; Pandey and Callomon 1995; Jain et al. 1996; Krishna et al. 1996a, b, 1998, 2000, 2009a, b, c; Kayal and Bardhan 1998; Alberti et al. 2011). Although the broad ages of the sedimentary units have been firmly established, there are still a few gaps in our knowledge. For example, no detailed succession of ammonite subzones for the Oxfordian has been suggested so far (Krishna et al. 2009a).

During two field surveys to the Kachchh Mainland concentrating on Oxfordian sediments several hundred ammonites have been collected from the measured sections. Unfortunately, the specimens are not evenly distributed throughout the sections, with several horizons being completely barren. Nevertheless, it has been possible to assign ages to the various lithostratigraphic units. These can be correlated easily throughout Kachchh Mainland, but obviously are not necessarily isochronous.

The Gypsiferous Shale member contains abundant ammonites and can be attributed to the Athleta Zone of the Late Callovian. The boundary to the next unit, the Dhosa Sandstone member, is diachronous. While the base of the Dhosa Sandstone in Lodai still yields ammonites indicative of the Athleta Zone (John H. Callomon pers. comm. 2000), in Jara and Jumara domes it is already Early Oxfordian in age. The lithological distinction between Dhosa Sandstone and Dhosa Oolite members is based solely on the presence of allochthonous, ferruginous ooids. Usually the Dhosa Oolite member follows on top of the Dhosa Sandstone member, but the occurrence of ooids is relatively arbitrary and both units are therefore, considered together. While the Lamberti Zone has not been found in the studied sections, both Mariae and Cordatum Zones have been recognized (John H. Callomon pers. comm. 2009). All studied belemnites from the Dhosa Sandstone and Dhosa Oolite are from the Cordatum Zone, as the Mariae Zone did not yield any belemnites.

The Dhosa Conglomerate Bed is highly fossiliferous and contains abundant ammonites reworked from several ammonite zones. This has been suggested already earlier on (e.g., Singh 1989). The youngest ammonites in the bed are from the Transversarium Zone of the Middle Oxfordian (Krishna et al. 1996b, 2009b, c). Deposition of the topmost unit, the Katrol Formation, started in the Alterneplicatus Zone of Early Kimmeridgian (equivalent to European Divisum Zone; Krishna et al. 1996a, 2009a). A large depositional gap between the Dhosa Conglomerate Bed and the Katrol Formation is apparent.

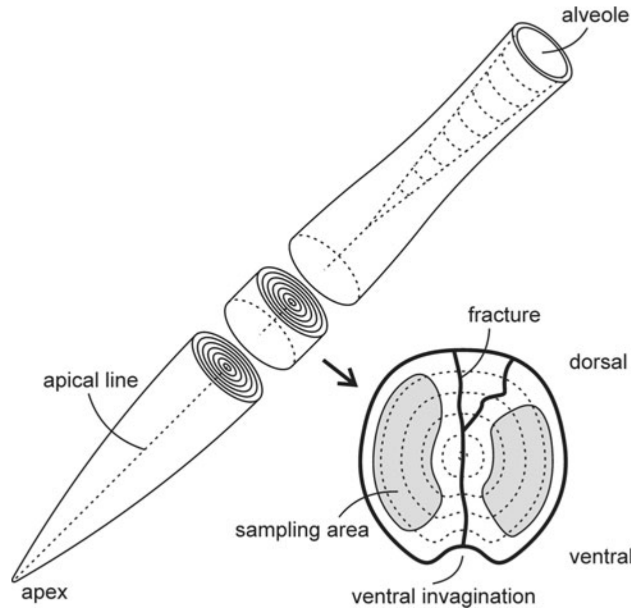

Fig. 4 Sample preparation of belemnite rostra for this study. An approximately 5–10-mm-thick slice has been cut from each rostrum and one side of it has been finely ground. The surface has been studied with cathodoluminescence microscopy to discern unaltered areas for sampling. Especially zones around the apical line, fractures, ventral invagination, and outer rim were prone to alteration by diagenetic fluids and therefore, avoided during sampling

Materials and methods

During the field surveys, more than 500 belemnites from different localities and various stratigraphic levels were collected. All rostra were examined macroscopically for signs of reworking, weathering or diagenetic alteration (bioerosion, abrasion, filled fractures, recrystallization, etc.) and the most promising specimens have been selected.

Sections of ca. 5–10 mm thickness were cut and their surfaces ground (Fig. 4). Each specimen was investigated using cathodoluminescence microscopy in order to test for diagenetic recrystallization. Operating conditions were an accelerating potential of around 15 kV and a beam current of ca. 400 μA. Only belemnite fragments with large non-luminescent areas were considered for further analyses.

Using a dental drill, the non-luminescent areas of the well-preserved belemnite sections were sampled retrieving between 5 and 15 mg of carbonate powder. The main part of the collected sample was consumed by the analysis of trace elements (Mn, Fe, Sr) using an ICP-AES after complete dissolution of the powder in 3% hydrochloric acid overnight. Each sample was measured at least twice to check reproducibility of the analyses. Furthermore, laboratory standards were measured regularly to check the calibration accuracy.

Less than 1 mg of carbonate powder was used for the stable isotope analysis. The samples were reacted with 100% H_3PO_4 at 75°C in an online, automated carbonate reaction device (Kiel III) connected to a ThermoFinnigan 252 mass spectrometer. All values are reported in per mil relative to V-PDB by assigning a δ^{13}C value of +1.95‰ and a δ^{18}O value of −2.20 ‰ to NBS19. During analyses, reproducibility was checked by replicate analyses of laboratory standards and was better than ± 0.06‰ for δ^{13}C and ± 0.07‰ for δ^{18}O.

Selected belemnite rostra were examined with a scanning electron microscope after 20 s etching with 1 n HCl. Only belemnites that were in no way suspicious of diagenetic alteration and could reliably be assigned to a biostratigraphic zone were used for drawing conclusions.

Results

The results of the trace element and stable isotope analyses are listed in Tables 1 and 2.

Cathodoluminescence microscopy

Cathodoluminescence microscopy revealed different degrees of preservation, not always congruent with the

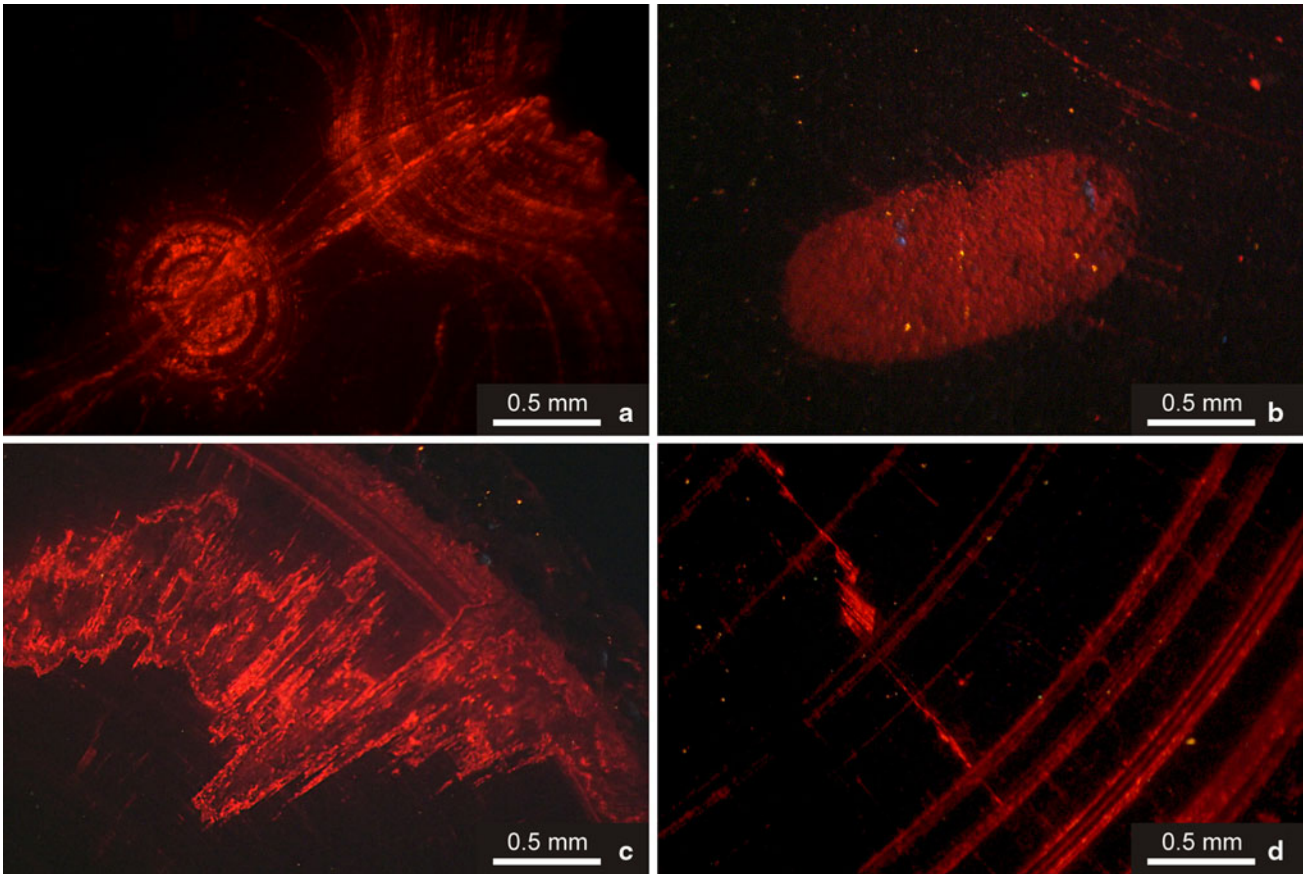

Fig. 5 Cathodoluminescence microscopy of belemnites from Kachchh Mainland. **a** Strong luminescence around apical line and ventral invagination, Dhosa Conglomerate Bed, Samatra, GZN2010I 1239. **b** Boring filled with strongly luminescent sediment in otherwise non-luminescent belemnite, silt on top of Dhosa Conglomerate Bed, Medisar, GZN2009II 957. **c** Broad fracture zone, Dhosa Oolite, Kotai, GZN2009II 963. **d** Thin fracture crosses luminescent growth lines, Dhosa Oolite, Jumara, GZN2009II 967

macroscopic investigations. Even few very dark, apparently well-preserved belemnites showed red–orange luminescence thought to be caused by Mn^{2+}, which entered the calcite crystals during diagenetic alteration (Fürsich et al. 2005; Wierzbowski et al. 2009). Characteristically, the outer rim of belemnites may show luminescence, especially strong around the ventral invagination. Additionally, the apical line served as a pathway for diagenetic fluids, which alter the isotopic signals (Fig. 5a). Common are fractures from the ventral invagination through the apical line towards the dorsal side (compare Fig. 10b). Such areas prone to diagenetic alteration were avoided during the sampling process. Fractures caused during retrieval of the belemnites in the field were easily distinguished from older ones, which show strong luminescence due to recrystallization (Fig. 5c, d). Few belemnites showed traces of bioerosion, whereby borings in the rostrum are filled with strongly luminescent sediment (Fig. 5b). After thorough microscopic examination the number of samples was reduced from 154 to 83.

Trace element analysis

Estimates for pristine trace element concentrations in the low-Mg calcite of belemnite rostra exist, which consider the ambient sea-water chemistry as well as biological fractionation processes (e.g., Wierzbowski and Joachimski 2007). However, during post depositional processes, in which pore waters interact with the fossil remains such as diagenesis or weathering, these trace elemental concentrations commonly can be altered. Typically, this leads to a decrease in Sr content as well as an increase in Fe and Mn (Price and Sellwood 1997; Wierzbowski and Joachimski 2007; Wierzbowski et al. 2009). Therefore, the measurement of Mn, Fe, and Sr allows the evaluation of the degree of diagenetic alteration.

To exclude altered samples cut-off grades were introduced for each of the three elements. Samples with Mn $>$ 100 ppm, Fe $>$ 300 ppm, and Sr $<$ 800 ppm were excluded from the dataset for interpretation (comparable with cut-off grades in Wierzbowski and Joachimski 2007;

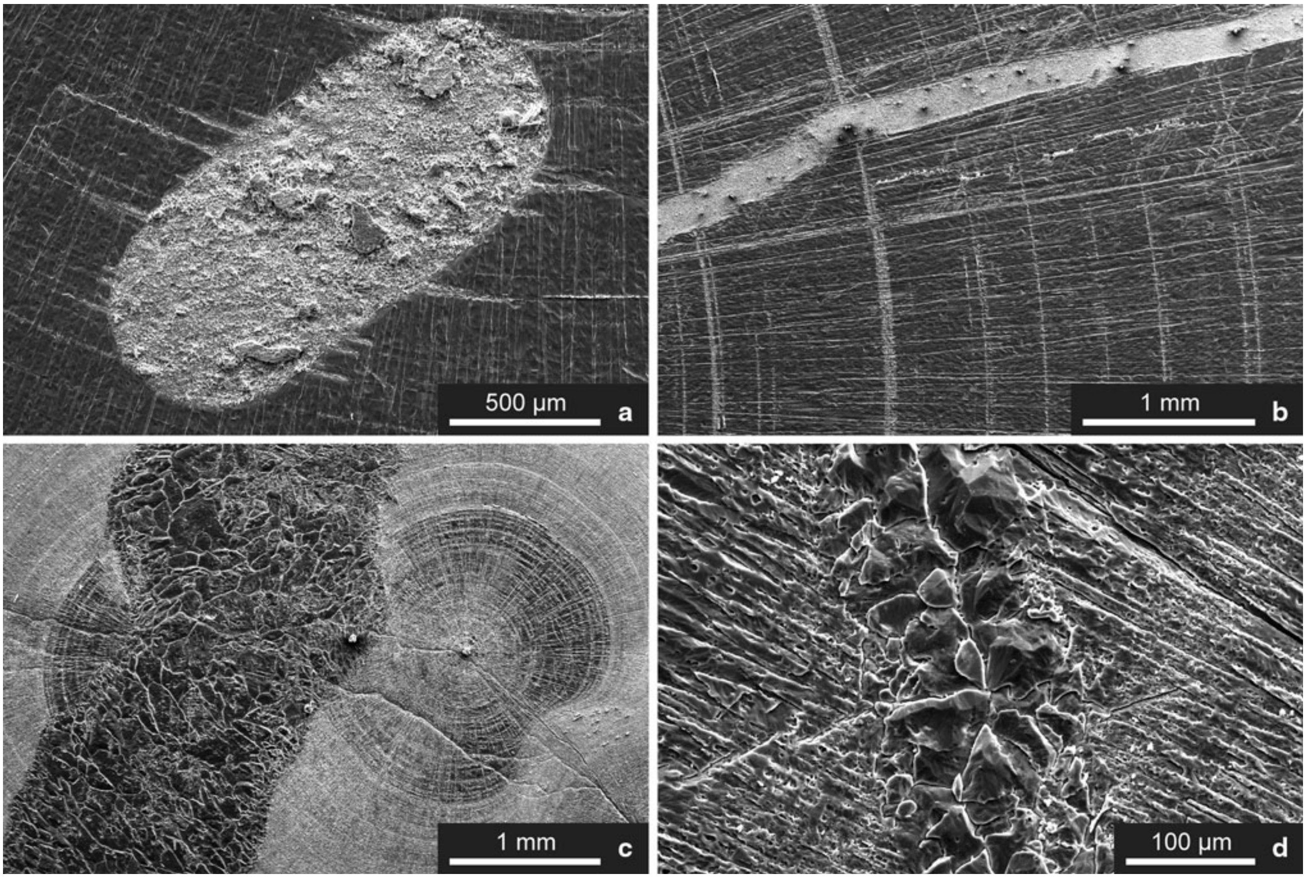

Fig. 6 Scanning electron microscopy of belemnites from Kachchh Mainland. Samples had been etched for 20 s with 1 n HCl. **a** Boring filled with sediment in otherwise relatively well preserved belemnite. Sediment extends into skeletal calcite along growth lines; silt on top of Dhosa Conglomerate Bed, Medisar, GZN2009II 957. **b** Thin fracture crossing growth lines of otherwise well preserved belemnite, Dhosa Conglomerate Bed, Kamaguna, GZN2009I 922. **c** Broad fracture zone in poorly preserved belemnite, Dhosa Sandstone, Keera, GZN2009II 950. **d** Thin fracture cutting through skeletal calcite crystals, Dhosa Sandstone, Keera, GZN2009II 950

Wierzbowski et al. 2009). This final step confined the number of reliable samples to 61. Table 1 lists the results from samples with trace element concentrations considered pristine, while Table 2 lists the results from the potentially altered samples.

Scanning electron microscopy

Selected belemnite samples were examined with a scanning electron microscope. Fractures crossing the rostra can easily be distinguished (Fig. 6b–d), but the distinction between altered and unaltered skeletal calcite crystals is not straightforward. Although most well-preserved belemnites contain large, uniform areas with radial calcite crystals and concentric growth lines, even some heavily altered specimens showing strong orange colors in cathodoluminescence microscopy may have quite similar features. In these cases, only a large number of fractures filled by recrystallized calcite reveal the poor state of preservation (Fig. 6c, d). Nevertheless, it is clear that this is not a very reliable criterion for evaluating the degree of alteration. The present study therefore, relied mostly on cathodoluminescence microscopy and trace element analyses. However, scanning electron microscopy may be useful for examining special features, such as bioerosion. As is visible under higher magnification, the sediment filling a boring extends into the surrounding skeleton along concentric growth lines (Fig. 6a).

Oxygen isotopes

The results of the oxygen isotope analyses are illustrated in Fig. 7.

Five reliable samples were retrieved from the Gypsiferous Shale member (Late Callovian) of Jhura, Jhuran and Fakirwari. Their δ^{18}O values range between −1.03 and −0.14‰. The δ^{18}O values of the three specimens from Jhura are very close together (−0.31 to −0.56‰; average: −0.45‰). The average of all five samples is −0.50‰.

Table 1 Results of trace element and stable isotope analyses from 61 reliable belemnite rostra of Kachchh Mainland

Sample	Unit[a]	Position[b] (m)	Stage	Ammonite zone[c]	Mn (ppm)	Fe (ppm)	Sr (ppm)	$\delta^{13}C$ (‰ V-PDB)	$\delta^{18}O$ (‰ V-PDB)	T (°C)[d]
Jara										
GZN2009II 943	Silt	+0.10	–	–	<33	242	1,327	−0.22	−0.04	12.1
GZN2009II 940	DCB	0	M.-L. Oxfordian	Transv.-Bif.	22	277	929	0.97	0.15	11.4
GZN2009II 930	DO	−0.15	E. Oxfordian	Cordatum	18	264	1,071	1.51	−0.74	14.9
GZN2009II 934	DO	−1.20	E. Oxfordian	Cordatum	<38	111	1,120	0.91	−0.70	14.8
Jumara										
GZN2009II 946	DO	−0.05	E. Oxfordian	Cordatum	<35	48	973	1.91	0.16	11.4
GZN2009II 926	DO	−0.25	E. Oxfordian	Cordatum	<42	102	968	1.52	0.12	11.5
GZN2009II 976	DO	−0.25	E. Oxfordian	Cordatum	<24	154	878	1.84	0.04	11.8
GZN2009II 978	DO	−0.25	E. Oxfordian	Cordatum	<42	221	1,126	0.64	0.02	18.0
GZN2009II 966	DO	−0.60	E. Oxfordian	Cordatum	<39	276	1,049	2.17	0.23	11.1
Medisar										
GZN2009II 957	Silt	+0.25	–	–	<41	<41	1,381	−0.24	−0.27	13.0
GZN2009II 1103	DCB	0	M.-L. Oxfordian	Transv.-Bif.	<39	161	1,002	1.39	0.25	11.0
GZN2009II 955	DO	−0.35	E. Oxfordian	Cordatum	<24	65	1,210	1.11	−0.73	14.9
Kamaguna										
GZN2009II 922	DCB	0	M.-L. Oxfordian	Transv.-Bif.	<34	<34	1,058	1.30	0.14	11.5
GZN2009II 921	DO	−0.40	E. Oxfordian	Cordatum	<41	112	955	2.12	0.03	11.9
GZN2009II 920	DO	−1.30	E. Oxfordian	Cordatum	<17	118	1,317	1.05	−0.24	12.9
Jhura										
GZN2010I 1226	DO	−0.25	E. Oxfordian	Cordatum	<17	60	1,149	0.27	−0.15	12.6
GZN2010I 1235	DO	−1.25	E. Oxfordian	Cordatum	<18	32	925	2.28	0.55	9.9
GZN2010I 1236	DO	−1.25	E. Oxfordian	Cordatum	<22	<22	1,201	1.19	−0.50	14.0
GZN2010I 1269	DO	−2.40	E. Oxfordian	Cordatum	<26	29	1,176	0.60	−0.91	15.6
GZN2010I 1209	DO	−4.90	E. Oxfordian	Cordatum	<18	33	1,174	1.08	−0.89	15.5
GZN2010I 1210	DO	−4.90	E. Oxfordian	Cordatum	<16	40	1,102	0.53	−0.51	14.0
GZN2010I 1205	DO	−6.00	E. Oxfordian	Cordatum	<22	<22	1,177	1.08	−0.59	14.3
GZN2010I 1288	GS	−16.10	L. Callovian	Athleta	<16	36	1,263	1.07	−0.31	13.2
GZN2010I 1289	GS	−16.10	L. Callovian	Athleta	<16	38	1,249	1.09	−0.48	13.9
GZN2010I 1290	GS	−16.10	L. Callovian	Athleta	26	130	1,154	0.99	−0.56	14.2
Kotai										
GZN2010I 1247	KA	+14.55	Kimmeridgian	≥Alterneplicatus	<30	109	1,369	−0.79	−0.05	12.2
GZN2010I 1264	KA	+9.45	Kimmeridgian	≥Alterneplicatus	<33	164	1,299	−1.26	−0.03	12.1
GZN2009II 962	DO	−1.95	E. Oxfordian	Cordatum	<43	273	1,019	1.52	0.00	12.0
GZN2009II 961	DO	−2.10	E. Oxfordian	Cordatum	<35	206	1,335	1.52	−0.69	14.7
GZN2010I 1271	DS	−2.75	E. Oxfordian	Cordatum	<15	<15	833	1.68	0.43	10.3
GZN2009II 959	DS	−2.85	E. Oxfordian	Cordatum	<17	135	923	2.09	0.31	10.8
GZN2009II 960	DS	−2.85	E. Oxfordian	Cordatum	<20	293	1,209	1.18	−0.77	15.1
GZN2010I 1267	DS	−5.25	E. Oxfordian	Cordatum	<29	<29	1,199	0.48	−0.43	13.7
Dhrang										
GZN2009II 1105	DO	−0.30	E. Oxfordian	Cordatum	<20	55	1,129	1.05	−1.10	16.4
GZN2010I 1262	DO	−0.85	E. Oxfordian	Cordatum	<23	71	1,325	1.86	−0.85	15.4
GZN2010I 1263	DO	−0.85	E. Oxfordian	Cordatum	<16	31	1,240	0.91	−0.60	14.4
GZN2009II 965	DS	−3.50	E. Oxfordian	Cordatum	<47	<47	1,139	0.98	−0.47	13.8
Lodai										
GZN2009II 1110	DCB	0	M.-L. Oxfordian	Transv.-Bif.	<31	<31	1,178	−0.05	0.37	10.6
GZN2009II 901	Slab	0	E. Oxfordian	Cordatum	<18	111	1,168	−0.15	−0.55	14.2

Table 1 continued

Sample	Unit[a]	Position[b] (m)	Stage	Ammonite zone[c]	Mn (ppm)	Fe (ppm)	Sr (ppm)	$\delta^{13}C$ (‰ V-PDB)	$\delta^{18}O$ (‰ V-PDB)	T (°C)[d]
GZN2010I 1248	DO	−6.25	E. Oxfordian	Cordatum	<23	<23	1,110	1.45	−0.68	14.7
Jhuran										
GZN2010I 1206	KA	+25.20	Kimmeridgian	≥Alterneplicatus	<23	59	1,221	−0.15	−0.14	12.5
GZN2010I 1213	KA	+11.60	Kimmeridgian	≥Alterneplicatus	<18	80	1,189	0.73	−0.11	12.4
GZN2010I 1215	KA	+7.90	Kimmeridgian	≥Alterneplicatus	<29	137	1,332	0.30	−0.19	12.7
GZN2010I 1233	DCB	0	M.-L. Oxfordian	Transv.-Bif.	<48	63	1,353	0.23	0.45	10.3
GZN2010I 1257	GS	−1.30	L. Callovian	Athleta	<22	28	1,298	0.09	−0.14	12.5
Samatra										
GZN2010I 1221	Crust	0	–	–	<33	204	1,244	−0.36	−0.49	13.9
GZN2010I 1222	Crust	0	–	–	<27	114	1,314	−0.40	−0.48	13.9
Mandvi Rd										
GZN2010I 1217	DS	−2.50	E. Oxfordian	Cordatum	<12	26	>1,179	0.87	−0.22	12.8
GZN2010I 1218	DS	−2.50	E. Oxfordian	Cordatum	<25	46	1,067	0.78	−0.90	15.6
Fakirwari										
GZN2010I 1253	KA	+2.55	Kimmeridgian	≥Alterneplicatus	<19	138	>1,897	−0.01	0.21	11.2
GZN2009II 1101	DCB	0	M.-L. Oxfordian	Transv.-Bif.	<18	121	1,094	0.61	0.42	10.4
GZN2009II 918	DCB	0	M.-L. Oxfordian	Transv.-Bif.	47	229	1,152	0.90	0.43	10.3
GZN2009II 913	DS	−0.75	E. Oxfordian	Cordatum	<16	124	1,200	0.31	−1.38	17.6
GZN2009II 914	DS	−0.75	E. Oxfordian	Cordatum	<18	64	1,205	0.07	−1.09	16.4
GZN2009II 912	DS	−0.95	E. Oxfordian	Cordatum	<17	82	1,428	0.18	−1.13	16.5
GZN2009II 911	DS	−1.25	E. Oxfordian	Cordatum	<19	120	1,229	0.33	−0.87	15.5
GZN2009II 910	DS	−1.25	E. Oxfordian	Cordatum	<20	193	972	2.77	− 0.55	14.2
GZN2009II 905	DS	−3.15	E. Oxfordian	Cordatum	<35	40	1,294	0.30	−0.96	15.8
GZN2009II 906	DS	−3.15	E. Oxfordian	Cordatum	<18	42	1,327	1.07	−0.62	14.5
GZN2009II 903	GS	−3.70	L. Callovian	Athleta	<15	129	1,492	0.79	−1.03	16.1
Ler										
GZN2010I 1256	KA	+3.50	Kimmeridgian	≥Alterneplicatus	<16	134	1,209	−0.45	−0.24	12.9

[a] *GS* Gypsiferous Shale member, *DS* Dhosa Sandstone member, *DO* Dhosa Oolite member, *DCB* Dhosa Conglomerate Bed, *KA* Katrol Formation

[b] The stratigraphic position is given in distance to the Dhosa Conglomerate Bed

[c] *Transv.* Transversarium, *Bif.* Bifurcatus

[d] Temperatures were calculated using the equation given by Anderson and Arthur (1983) and a $\delta^{18}O$ value for seawater of −1‰ V-SMOW for an ice-free Jurassic world

The majority of the samples (~61%) comes from the Dhosa Sandstone and Dhosa Oolite members (Early Oxfordian). The $\delta^{18}O$ values range between −1.38 and 0.55‰, the average being −0.47‰.

Seven samples were analyzed from the matrix of the Dhosa Conglomerate Bed (Middle-Late Oxfordian) of Jara, Medisar, Kamaguna, Lodai, Jhuran, and Fakirwari. Their $\delta^{18}O$ values range between 0.14 and 0.45‰ with an average of 0.32‰. The two samples from Fakirwari show very close $\delta^{18}O$ values (0.42 and 0.43‰).

Both samples from Samatra belong to a thin sediment layer at the top of the conglomerate ("crust") and are not representative of the actual Dhosa Conglomerate Bed. Since no more samples from the same level at other sections have been measured, and both samples are the only ones from Samatra, they have not been used for further interpretation.

One belemnite from a reworked, concretionary slab of oolitic fine-grained sandstone floating within the Dhosa Conglomerate Bed has been analyzed from Lodai. With a $\delta^{18}O$ value of −0.55‰ it very well fits the values from beds underneath the Dhosa Oolite member to which the slab most likely belongs.

Two samples belong to the silty unit on top of the Dhosa Conglomerate Bed, whose litho- and biostratigraphic assignment is still pending. The $\delta^{18}O$ values of these samples from Jara and Medisar are −0.04 and −0.27‰.

Seven samples from the Katrol Formation (Kimmeridgian) of Kotai, Jhuran, Fakirwari, and Ler were analyzed.

Table 2 Results of trace element and stable isotope analyses of samples that were removed from the dataset because of possible alteration of isotope and trace element content (*italicized cells* indicate values above, respectively below cut-off grades: Mn > 100 ppm, Fe > 300 ppm, Sr < 800 ppm)

Sample	Unit[a]	Position[b] (m)	Stage	Ammonite zone[c]	Mn (ppm)	Fe (ppm)	Sr (ppm)	δ^{13}C (‰ V-PDB)	δ^{18}O (‰ V-PDB)	T (°C)[d]
Jara										
GZN2009II 942	Silt	+0.10	–	–	<26	*320*	1,351	0.16	0.04	11.8
GZN2009II 938	DCB	0	M.-L. Oxfordian	Transv.-Bif.	37	*692*	1,254	−0.87	−6.22	41.1
GZN2009II 933	DO	−0.05	E. Oxfordian	Cordatum	*490*	*1,028*	1,141	−0.13	−3.31	26.3
GZN2009II 929	DO	−0.15	E. Oxfordian	Cordatum	45	*401*	970	0.76	−1.05	16.2
Jumara										
GZN2009II 969	DCB	0	M.-L. Oxfordian	Transv.-Bif.	<34	*608*	1,481	0.08	−0.07	12.3
GZN2009II 970	DCB	0	M.-L. Oxfordian	Transv.-Bif.	<17	*> 1,660*	1,298	−0.12	0.00	12.0
GZN2009II 971	DCB	0	M.-L. Oxfordian	Transv.-Bif.	<22	*534*	1,164	−0.57	−0.30	13.2
GZN2009II 974	DCB	0	M.-L. Oxfordian	Transv.-Bif.	31	*421*	975	0.77	−0.54	14.1
GZN2009II 975	DCB	0	M.-L. Oxfordian	Transv.-Bif.	<63	*436*	1,108	0.79	0.20	11.2
GZN2009II 927	DO	−0.25	E. Oxfordian	Cordatum	69	*452*	1,125	1.56	−1.34	17.4
GZN2009II 979	DO	−0.25	E. Oxfordian	Cordatum	<20	*856*	903	2.41	−0.23	12.9
Medisar										
GZN2009II 958	Silt	+0.25	–	–	<34	*781*	1,300	−0.08	0.03	11.9
Kamaguna										
GZN2009II 923	DCB	0	M.-L. Oxfordian	Transv.-Bif.	<52	*302*	955	1.17	−0.47	13.8
Jhura										
GZN2009II 982	DO	−0.25	E. Oxfordian	Cordatum	<60	*469*	1,129	0.74	−1.60	18.5
GZN2010I 1225	DO	−0.25	E. Oxfordian	Cordatum	<23	*302*	1,166	−0.23	−0.05	12.2
GZN2009II 981	DO	−5.80	E. Oxfordian	Cordatum	<23	*380*	1,159	0.21	−3.51	27.2
Rudra Mata										
GZN2009II 954	DCB	0	M.-L. Oxfordian	Transv.-Bif.	<27	*426*	1,040	0.97	−1.49	18.1
Kotai										
GZN2009II 964	DO	−0.40	E. Oxfordian	Cordatum	<55	*396*	953	1.10	−0.33	13.3
Mandvi Rd										
GZN2010I 1216	DS	−2.50	E. Oxfordian	Cordatum	<28	*393*	1,298	1.06	−0.63	14.5
Fakirwari										
GZN2009II 915	DS	−0.55	E. Oxfordian	Cordatum	42	*887*	*597*	0.44	−4.47	32.0
GZN2009II 908	DS	−2.05	E. Oxfordian	Cordatum	<54	*432*	1,375	−0.77	−1.19	16.8
GZN2009II 909	DS	−2.05	E. Oxfordian	Cordatum	<13	*343*	1,201	0.21	−2.60	23.0

[a] *GS* Gypsiferous Shale member, *DS* Dhosa Sandstone member, *DO* Dhosa Oolite member, *DCB* Dhosa Conglomerate Bed, *KA* Katrol Formation

[b] The stratigraphic position is given in distance to the Dhosa Conglomerate Bed

[c] *Transv.* Transversarium, *Bif.* Bifurcatus

[d] Temperatures were calculated using the equation given by Anderson and Arthur (1983) and a δ^{18}O value for seawater of −1‰ V-SMOW for an ice-free Jurassic world

Their δ^{18}O values range between −0.24 and 0.21‰ with an average of −0.08‰. Values of samples from the same locality plot closely together (Kotai: −0.05 to −0.03‰; Jhuran: −0.19 to −0.11‰).

Possibly more important than the absolute values of the δ^{18}O analyses are the trends visible in the sections. As we follow the isotope curves from the Gypsiferous Shale member upwards we see relatively stable conditions throughout the units with only few perturbations (such as around the boundary of the Dhosa Sandstone and Dhosa Oolite member in Kotai). These perturbations are restricted to single sections and cannot be correlated from one section to another. Striking is an increase in δ^{18}O values (corresponding to a drop in paleotemperature) at the boundary to the Dhosa Conglomerate Bed, which can be seen throughout Kachchh Mainland. The values of the strata on

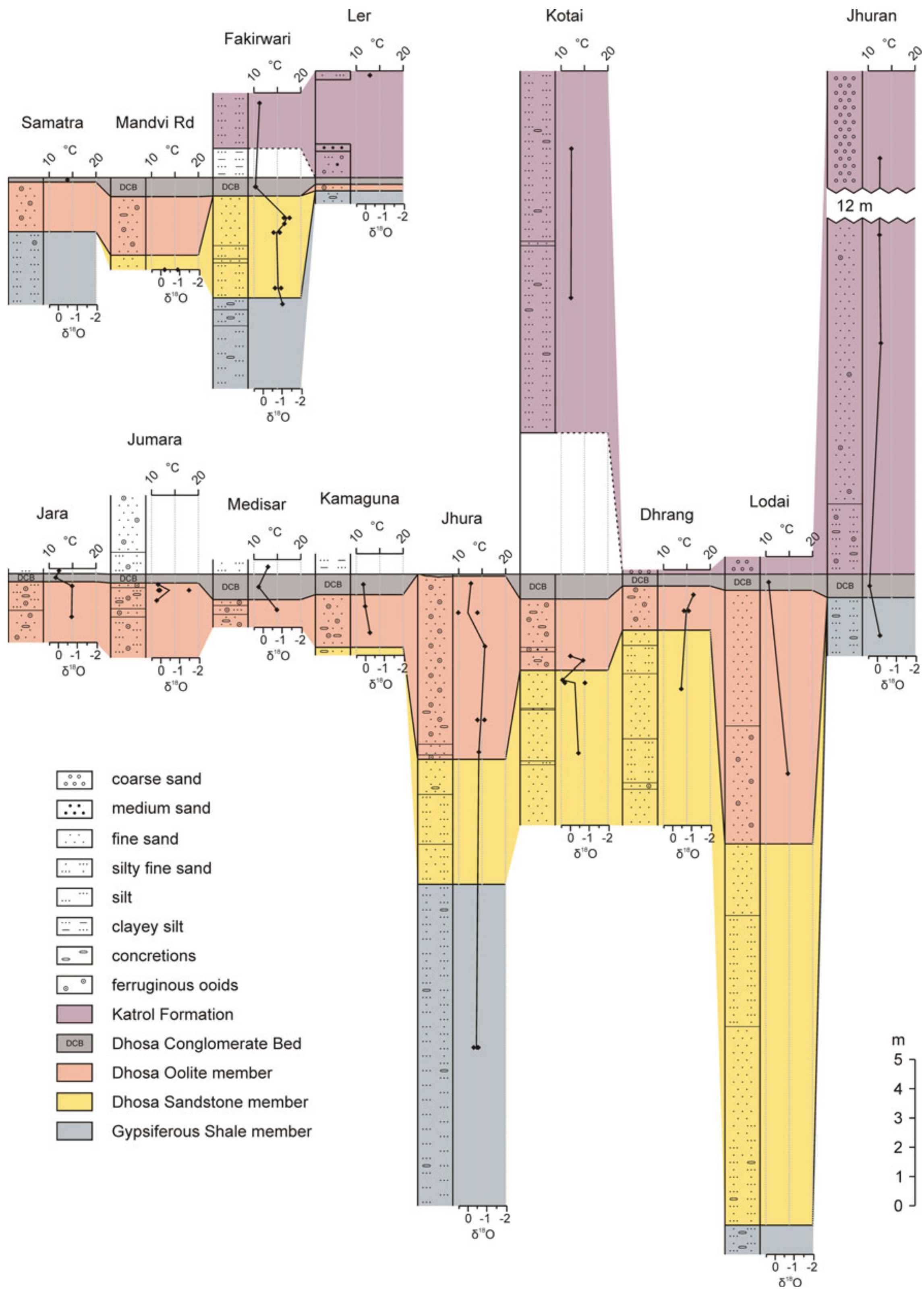

Fig. 7 Results of the oxygen isotope analyses for all sections yielding reliable samples ($\delta^{18}O$ values are given in ‰ V-PDB). For the location of the sections, see Figs. 1 and 8

top are again more negative even though they do not reach the average of the units from the Gypsiferous Shale to the Dhosa Oolite member.

Carbon isotopes

The results of the carbon isotope analyses are illustrated in Fig. 8.

The $\delta^{13}C$ values of the five samples from the Gypsiferous Shale member (Late Callovian) range between 0.09 and 1.09‰ with an average of 0.81‰. The samples from Jhura show very similar values (0.99 to 1.09‰). The 37 samples from the Dhosa Sandstone and Dhosa Oolite members (Early Oxfordian) have $\delta^{13}C$ values ranging from 0.07 to 2.77‰ with an average of 1.17‰. The $\delta^{13}C$ values of the seven samples from the matrix of the Dhosa Conglomerate Bed (Middle-Late Oxfordian) range between −0.05 and 1.39‰ with an average of 0.76‰. The two samples from the "crust" at the top of the Dhosa Conglomerate Bed from Samatra show $\delta^{13}C$ values of −0.40 and −0.36‰. The $\delta^{13}C$ value of the single belemnite from the concretionary slab in the Dhosa Conglomerate Bed is −0.15‰. The silty unit on top of the Dhosa Conglomerate Bed produced two samples with $\delta^{13}C$ values of −0.24 and −0.22‰. The $\delta^{13}C$ values of the seven samples from the Katrol Formation (Kimmeridgian) range between −1.26 and 0.73‰ with an average of −0.23‰. The values scatter very much and contrary to the results of the $\delta^{18}O$ analysis even samples from the same locality have strongly variable $\delta^{13}C$ values (Jhuran: −0.15 to 0.73‰).

The results of the $\delta^{13}C$ isotope analyses are less clear than those of the $\delta^{18}O$ analyses. Relatively stable conditions can be seen in the lower units, from the Gypsiferous Shale up to the Dhosa Oolite member. The Dhosa Conglomerate Bed has, in general, slightly lower $\delta^{13}C$ values, but in a few sections (Medisar, Jhuran, and Fakirwari) $\delta^{13}C$ values even increase. Striking though is the large drop in $\delta^{13}C$ values on top of the Dhosa Conglomerate Bed with almost exclusively negative values.

Figure 9 shows that there is no correlation between $\delta^{18}O$ and $\delta^{13}C$ values (correlation coefficient $R = 0.12$). This suggests that no kinetic fractionation influenced the isotope compositions (Fürsich et al. 2005).

It has been found that stable isotope values of belemnites from the same stratigraphic horizon can scatter considerably (occasionally up to 1‰; compare Veizer et al. 1999; McArthur et al. 2007; Mutterlose et al. 2010). In the present study this holds true especially for the $\delta^{13}C$ values, which is why a large number of samples is necessary to obtain reliable trends. The data from the Kachchh Basin is not easy to interpret in this context. The global Middle Oxfordian $\delta^{13}C$ maximum event described by several authors from the Plicatilis-Transversarium Zone (Jenkyns 1996; Weissert and Mohr 1996; Wierzbowski 2002; Pearce et al. 2005; Louis-Schmid et al. 2007) has not been found in our samples. This could be due to the condensed nature of the Dhosa Conglomerate Bed, which precludes a high biostratigraphic resolution. Possibly, belemnites representing this time interval do not occur in the unit, which is characterized by a series of depositional gaps. Striking is the decrease of $\delta^{13}C$ values towards the Early Kimmeridgian. This is comparable to data of Brigaud et al. (2008) from the Paris Basin, who also described lowest values from the Early Kimmeridgian and could not find the Middle Oxfordian maximum.

Discussion

Diagenetic alteration and reworking

Diagenetic alteration can lead to changes in elemental concentrations and isotope composition of belemnites. Cathodoluminescence microscopy as well as trace element analysis proved to be a very effective means of excluding diagenetically altered samples from the dataset. From 154 macroscopically selected belemnites only 61 passed all tests. It is suggested that even most of the neglected samples provide valid, primary isotope signatures as can be seen by many reasonable values in Table 2. Nevertheless, to improve the reliability of the isotope signatures only samples, which are in no way suspicious of diagenetic alteration, have been included in the dataset.

The aim of this study was to gather isotope curves from sections exposing the Middle to Late Jurassic transition throughout Kachchh Mainland. However, several outcrops did not yield unaltered belemnites. Because of intense weathering, all belemnite samples from Keera Dome and Rudra Mata (Habo Dome) were excluded. At many outcrops belemnites showed high degrees of weathering at certain stratigraphic levels. After excluding these altered samples, some sections were left with only one or two reliable isotope data. Nevertheless, it has been possible to produce meaningful isotope curves for a series of sections from the most proximal areas of the basin exposed on Kachchh Mainland at Jhuran to the more distal Jara and Jumara domes.

As the abundant ammonites in the Dhosa Conglomerate Bed are reworked the question whether the belemnites within the layer are autochthonous or not has to be addressed. While signs of reworking of belemnites are relatively rare in underlying strata, heavily bored or recrystallized specimens are common in the Dhosa Conglomerate Bed (Fig. 10d). There are, however, also well-preserved specimens that seem to have been exposed on the

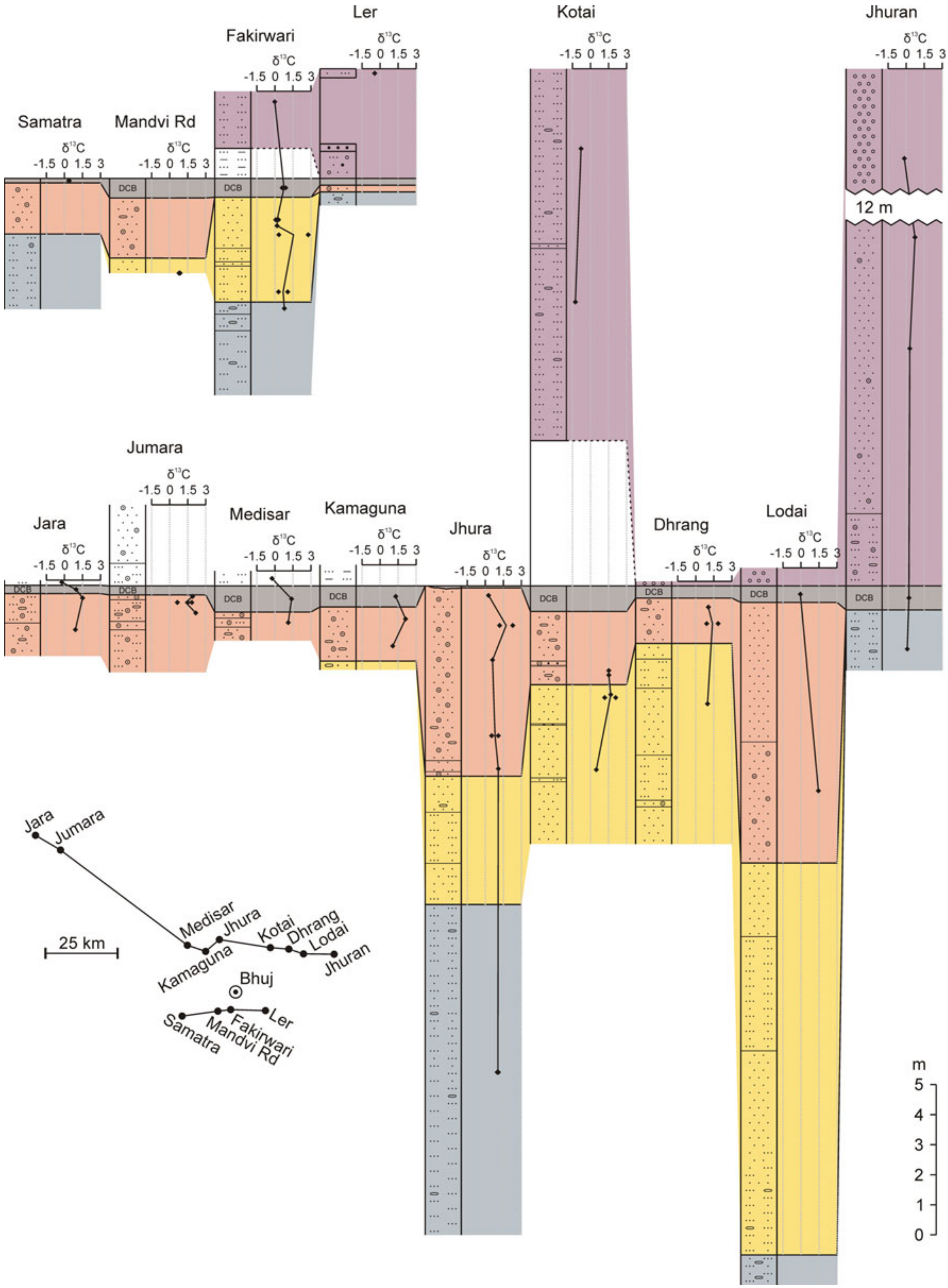

Fig. 8 Results of the carbon isotope analyses for all sections yielding reliable samples (δ^{13}C values are given in ‰ V-PDB). The small map shows the relative position of the localities on Kachchh Mainland. For legend, see Fig. 7

sea floor only for a short period before final burial. They have been bored only at the outermost rim if at all and the borings have very sharp boundaries (Fig. 10a, c).

It seems that there are two groups of belemnites in the Dhosa Conglomerate Bed; one consists of reworked specimens, which are strongly altered, the other comprises

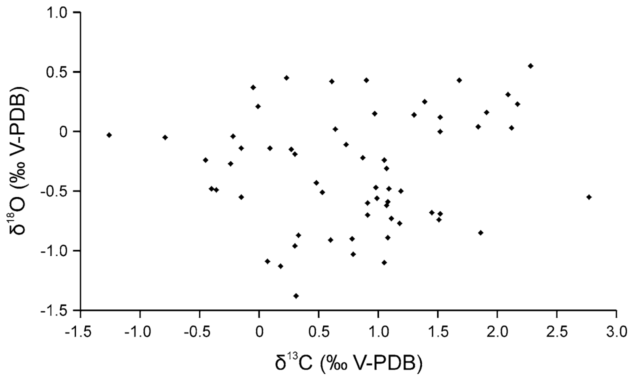

Fig. 9 δ^{18}O versus δ^{13}C values of well-preserved belemnites from Kachchh Mainland. No significant correlation has been found ($R = 0.12$)

more or less well-preserved specimens that underwent only minor reworking. It is therefore, possible to retrieve reliable isotope information from the Dhosa Conglomerate Bed, but considerable attention has to be paid to choose the right specimens. Owing to these difficulties, a larger amount of samples from the Dhosa Conglomerate Bed has been examined (and also rejected) to obtain unaltered specimens for analysis. Usually diagenetic alteration leads to an increase in the calculated paleotemperatures (e.g., Brigaud et al. 2008; compare also data in Table 2). Since the temperatures from the Dhosa Conglomerate Bed are among the lowest in the dataset, it can be inferred that the sampled belemnites show pristine isotope composition. The analyzed belemnites are therefore, younger than most or even all of the reworked ammonites and are consequently assigned to the Transversarium-Bifurcatus zones (late Middle to early Late Oxfordian).

Belemnites as temperature indicators

Stable isotope analyses of belemnites have been used for paleoclimatic reconstructions since several decades (e.g., Urey et al. 1951). This is mainly due to their widespread occurrence and the relatively large amount of low-Mg calcite available for sampling. It is generally believed that belemnites precipitated their rostrum in oxygen isotope equilibrium with the surrounding water body (Tan et al. 1970; Price and Sellwood 1997; Wierzbowski and Joachimski 2007, 2009). Since the group became extinct at the end of the Cretaceous this assumption cannot be proven. The fact that modern cephalopods such as *Nautilus* precipitate their shells in equilibrium (Taylor and Ward 1983) has to suffice. Even if belemnites would show vital fractionation, inferred temperature trends should remain the same only having different absolute values.

Belemnites are widely regarded as nektonic organisms (Price and Sellwood 1997; Mutterlose et al. 2010). Large fossil concentrations on bedding planes, commonly known as belemnite battlefields, have been interpreted as post-spawning mass mortality (Doyle and MacDonald 1993). These accumulations demand migrations to spawning grounds, which agrees well with the morphology of belemnites similar to many modern squid species living as fast swimmers in the water column. Fürsich et al. (2005) suggested such migrations from cooler areas to explain why temperatures calculated from belemnites are often lower than those from benthic bivalves or brachiopods, although they should record higher temperatures living as nektonic organisms in the upper part of the water column. Furthermore, results by Dera et al. (2011) show that isotope trends recorded by belemnites and bivalves can be very different. Bivalves generally record higher temperatures and more fluctuations, which would be expected from shallower areas (Dera et al. 2011). Recently, a nektobenthic life style of belemnopseid belemnites has been suggested (Wierzbowski and Joachimski 2007, 2009; Wierzbowski et al. 2009). Although a nektobenthic mode of life has been proposed for some belemnites based on oxygen isotope data (Anderson et al. 1994), the results of Fürsich et al. (2005) do not support such interpretations for the species from the Kachchh Basin.

Specific identification of the analyzed belemnites has been hampered by the fact that most specimens are preserved or have been retrieved as fragments only. Nevertheless, based on the study of Late Jurassic belemnites from the Kachchh Basin by Desai and Patel (2009), most fragments could be easily assigned to the genera *Belemnopsis* and *Hibolithes*, both belonging to the family Belemnopseidae. The two genera have been reported to carry similar isotope signals (Price and Sellwood 1997; Wierzbowski and Joachimski 2007; Wierzbowski et al. 2009), which negates potential biases due to the use of several belemnite species (e.g., through different life habitats).

The Jurassic greenhouse world was characterized by much stronger precipitation than at present-day (Sellwood and Valdes 2006). However, these rain falls were restricted mainly to oceanic areas while large arid regions existed on the continents (Sellwood and Valdes 2006). Especially in coastal areas or enclosed basins this freshwater influx may have depleted surface waters in δ^{18}O, thereby influencing the stable isotope composition of faunal elements. Price and Sellwood (1997) assumed this process to be responsible for the very high temperatures of 17–18°C of Late Jurassic belemnites from the Falkland Plateau. Since the belemnites analyzed in the present study record lower temperatures than benthic organisms (Fürsich et al. 2005), it is not likely that they have been living close to the surface or were influenced by freshwater in the Kachchh Basin.

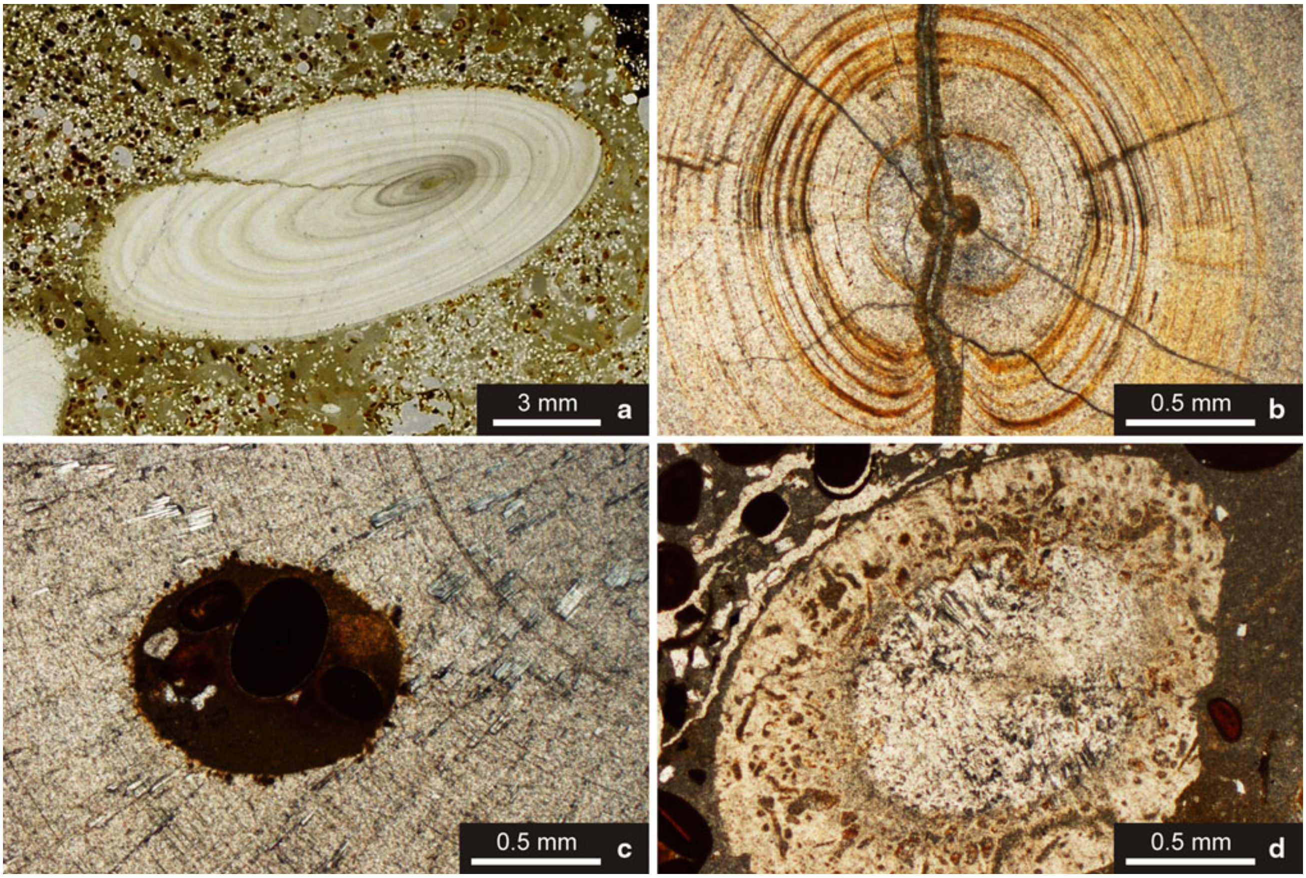

Fig. 10 Thin-sections of belemnites from Kachchh Mainland. **a** Moderately well preserved belemnite from the Dhosa Conglomerate Bed, Lodai. **b** Belemnites are often fractured across the apical line; slab in Dhosa Conglomerate Bed, Fakirwari. **c** Boring in otherwise moderately well preserved belemnite from the Dhosa Conglomerate Bed, Fakirwari. **d** Heavily bored, abraded, and recrystallized reworked belemnite from the Dhosa Conglomerate Bed, Fakirwari

Paleotemperatures in the Kachchh Basin

Paleotemperatures (Figs. 7, 11) were calculated using the equation given by Anderson and Arthur (1983). Assuming an ice-free world for the Jurassic, a δ^{18}O for seawater of −1‰ V-SMOW has been used (Shackleton and Kennett 1975). Only belemnites with reliable isotope compositions that could be assigned to biostratigraphic zones confidently were used for interpretation.

Late Callovian–Early Oxfordian

Temperatures calculated from the Late Callovian (Athleta Zone; Gypsiferous Shale member) and the Early Oxfordian (Cordatum Zone; Dhosa Sandstone and Dhosa Oolite members) are relatively stable and centered around 14°C. The most complete isotope curves for this time interval are from Jhura and Fakirwari, both of which do not show significant temperature excursions. Temperature variations can be seen only in very few sections such as Kotai, which shows large changes during the Early Oxfordian between samples from stratigraphically closely adjacent horizons. As these excursions cannot be correlated throughout the basin, they are thought to be only of minor significance.

Middle–Late Oxfordian

Belemnites of the Dhosa Conglomerate Bed show lower paleotemperatures than the underlying strata. This temperature decrease of more than 3°C down to an average of 10.8°C can be seen in all six sections from which data for the Dhosa Conglomerate Bed and lower beds are available. Ammonites from this unit are often reworked and belong to several ammonite zones from the Early to Middle Oxfordian. The belemnites used for the isotope analyses have been carefully selected and show no traces of reworking. Therefore, they should be of late Middle or even early Late Oxfordian age (Transversarium-Bifurcatus zones).

Kimmeridgian

The coarse sandstones of the Kimmeridgian (Katrol Formation) contain belemnites, which again yield higher

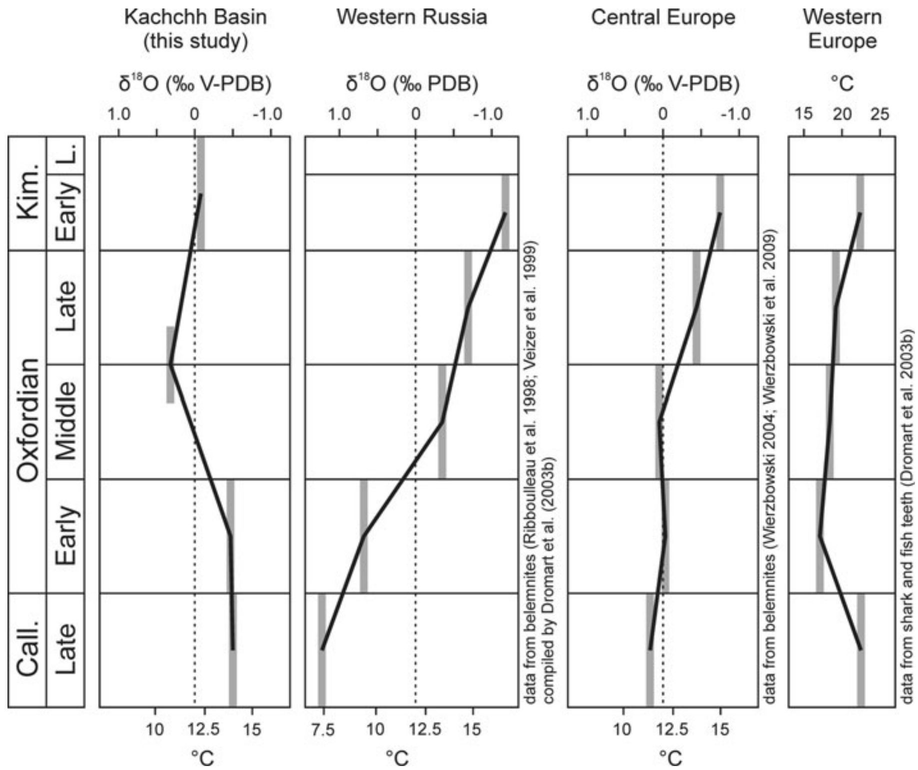

Fig. 11 Comparison of the results of the oxygen isotope analyses from Kachchh Mainland with results from other regions (data from Riboulleau et al. 1998; Veizer et al. 1999; Dromart et al. 2003b; Wierzbowski 2004; Wierzbowski et al. 2009). Average values for the $\delta^{18}O$ measurements of each time slice (*shown in grey*) have been calculated and connected

temperatures. The average temperature calculated is 12.3°C, which means an approximate increase in average temperature of 1.5°C since the Middle to Late Oxfordian.

Global paleoclimatic implications

Recently, the Middle to Late Jurassic transition (Callovian-Oxfordian boundary) has attracted attention due to the assumption of a glacial phase by Dromart et al. (2003a, b). These authors combined results from faunal, sedimentological, and isotope analyses for their hypothesis. The formation of polar glaciations calls for a global decrease in sea level and water temperatures.

A series of models for the Jurassic climate has been established over the last years (e.g., Valdes and Sellwood 1992; Valdes 1993; Price and Sellwood 1997; Sellwood et al. 2000; Sellwood and Valdes 2006). Although some of these reconstructions differ considerably (compare Valdes 1993), most of them point to equable conditions with no major global climatic changes (Sellwood and Valdes 2006). The whole Jurassic period seems to have been free of polar ice caps (Valdes and Sellwood 1992). Although Sellwood et al. (2000) mentioned the possibility of permafrost on the southern continents (Antarctica, India, and Australia), eustatic sea-level changes caused by glaciations seem unlikely for the Jurassic (Hallam 2001). The greenhouse climate was considerably warmer than today with sea-surface temperatures about 6°C higher (Valdes and Sellwood 1992) and temperatures on the ocean floor as high as 8°C (Sellwood and Valdes 2006). While these established climate models strongly contradict the hypothesis of Dromart et al. (2003a, b), they fit the data from the Kachchh Basin.

Although results of oxygen isotope analyses can vary regionally, an increase in paleotemperatures from the Late Callovian to the Early Kimmeridgian has been documented by several authors (e.g., Malchus and Steuber 2002; Rais et al. 2007; Brigaud et al. 2008; Dera et al. 2011), which disagrees with the hypothesis of Dromart et al. (2003a, b). In Fig. 11, the oxygen isotope data from the Kachchh Basin is compared with results from other studies. Belemnite rostra from western Russia compiled by Dromart et al. (2003b), Riboulleau et al. (1998), and Veizer et al. (1999) seem to show a more or less constant temperature rise from the Late Callovian to the Early Kimmeridgian. Only shark and fish teeth from Western Europe analyzed by Dromart et al. (2003b) show a distinct temperature decrease around the Callovian-Oxfordian boundary. A compilation from Wierzbowski (2004) and Wierzbowski et al. (2009) of data from belemnite rostra of central Europe shows relatively stable conditions from the Late Callovian to the Middle Oxfordian, followed by a steady increase in temperatures until the Early Kimmeridgian. The most exhaustive compilation of $\delta^{18}O$ data available at the moment for the Jurassic can be found in the study by Dera et al. (2011). Their belemnite data from the northwestern Tethys show a temperature minimum around the Middle to Late Callovian boundary, but at the Callovian to Oxfordian transition temperatures are already increasing again and continue to do so until the Early Kimmeridgian.

Paleotemperatures from the Early Callovian of the Kachchh Basin reported by Fürsich et al. (2005) center around 16.5°C. The belemnite rostra from Late Callovian and Early Oxfordian rocks analyzed in the present publication yield temperatures around 14°C. The Callovian of the Kachchh Basin is therefore, characterized by a temperature decrease, but this came already to a halt in the Athleta Zone of the Late Callovian. There is no sign of a distinct temperature change around the Middle to Late Jurassic transition. This observation disagrees with the hypothesis of Dromart et al. (2003a, b), which calls for a global temperature decrease around this boundary. In contrast, a distinct temperature drop has been recorded in the Kachchh Basin at the end of the Middle Oxfordian. Since most studies from other areas (including Dera et al. 2011) show more or less increasing temperatures during the Oxfordian, this decrease is suggested to be only a regional feature affecting the Kachchh Basin and possibly the Malagasy Gulf.

Dromart et al. (2003a) described sedimentary evidence of a sea-level fall of 40–80 m from localities around the world (e.g., condensed Upper Callovian sediments showing signs of subaerial erosion from Spain). On Kachchh Mainland the Callovian/Oxfordian boundary is characterized by a gradual shift from argillaceous silt (Gypsiferous Shale member) to cross-bedded fine sand (Dhosa Sandstone member). While this suggests a slight relative sea-level fall and higher energy conditions, it does not by far reach the magnitude proposed by Dromart et al. (2003a). Furthermore, Wierzbowski et al. (2009) challenged some of the arguments given by Dromart et al. (2003a) by reinterpreting the condensed Upper Callovian sediments from Spain as having formed through sediment starvation caused by a maximum transgression.

Conclusions

One hundred and fifty-four belemnite rostra from the Upper Callovian to Lower Kimmeridgian of the Kachchh Basin were checked by cathodoluminescence microscopy, trace element analysis and scanning electron microscopy. This strict selection process proved effective in excluding specimens with potentially altered isotope compositions from the dataset and produced 61 reliable samples showing pristine conditions. Paleotemperatures were calculated to evaluate climatic changes from the Late Callovian to the Kimmeridgian.

The obtained dataset has been compared with results of other authors, primarily Dromart et al. (2003a, b), who suggested polar glaciations around the Middle to Late Jurassic transition. Paleotemperatures calculated from belemnite rostra from the Kachchh Basin do not distinctly change at this boundary, but remain around 14°C. This is comparable with data from central Europe (Wierzbowski 2004; Wierzbowski et al. 2009), but does not favor the global temperature decrease proposed by Dromart et al. (2003a, b). While the sediments across the Callovian-Oxfordian boundary in the Kachchh Basin point to a gradual decrease in relative sea level connected with slightly higher energy levels, the magnitude is by far less than the sea-level fall of 40–80 m proposed by Dromart et al. (2003a). Furthermore, the relative sea-level minimum in the basin is reached in the Cordatum Zone of late Early Oxfordian and not at the boundary. The results from the Kachchh Basin therefore, do not show any evidence of polar glaciations that would have necessarily led to global sea-level and temperature fluctuations.

A pronounced temperature decrease of more than 3°C is inferred for the water body of the Kachchh Basin at the end of the Middle Oxfordian. Although the temperature drop seems to have occurred rapidly, this might be the result of the condensed nature of the Middle Oxfordian sediments. Further stable isotope studies on the expanded Jurassic sections of Wagad Island situated in the eastern part of the Kachchh Basin will help to pinpoint the exact biostratigraphic position and extent of this temperature decrease. As of now, stable isotope analyses from localities along the Malagasy Gulf are extremely rare for the Jurassic. Comparisons with data from such localities will help to determine whether this temperature minimum is only a local feature and restricted to the Kachchh Basin or possibly affected a larger region.

Acknowledgments The authors thank Michael Joachimski, Daniele Lutz, and Ulrike Wacker for support with stable isotope analyses. Ramona Dotzler and Heike Schmidt helped in preparing the samples. Birgit Leipner-Mata prepared the thin-sections. Christian Schulbert and Patrick Chellouche assisted with taking photographs at the scanning electron microscope. John Huntley helped with statistics. Financial support has been granted by the German Research Society (FU 131/34-1). The manuscript has been improved following suggestions of an anonymous reviewer and the editor Andre Freiwald.

References

Agrawal SK, Pandey DK (1985) Biostratigraphy of the Bathonian-Callovian beds of Gora Dongar in Pachchham "Island", District Kachchh (Gujarat). Proc Indian Natl Sci Acad Part A 51:887–903

Alberti M, Pandey DK, Fürsich FT (2011) Ammonites of the genus *Peltoceratoides* Spath, 1924 from the Oxfordian of Kachchh, western India. N Jb Geol Paläont Abh 262:1–18

Anderson TF, Arthur MA (1983) Stable isotopes of oxygen and carbon and their application to sedimentological and paleoenvironmental problems. In: Arthur MA, Anderson TF, Kaplan IR, Veizer J, Land L (eds) Stable isotopes in sedimentary geology. SEPM Short Course 10:1–151

Anderson TF, Popp BN, William AC, Ho LZ, Hudson JD (1994) The stable isotopic records of fossils from the Peterborough Member, Oxford Clay Formation (Jurassic), UK: palaeoenvironmental implications. J Geol Soc London 151:125–138

Bardhan S, Datta K (1987) Biostratigraphy of Jurassic Chari Formation: a study in Keera Dome, Kutch, Gujarat. J Geol Soc India 30:121–131

Bardhan S, Bhattacharya D, Mitra KC (1979) Significance of ammonite genus *Reineckeia* in the regional stratigraphic set-up of Jurassic of Kutch, Gujarat. Quart J Geol Min Metall Soc India 51:163–165

Bardhan S, Datta K, Khan D, Bhaumik D (1988) Tulitidae genus *Bullatimorphites* from Upper Bathonian Patcham Formation, Kutch, India. Newsl Strat 20:21–27

Biswas SK (1982) Rift basins in the western margin of India and their hydrocarbon prospects with special reference to Kutch Basin. Am Assoc Pet Geol Bull 66:1497–1513

Biswas SK (1991) Stratigraphy and sedimentary evolution of the Mesozoic basin of Kutch, western India. In: Tandon SK, Panz CC, Casshyap SM (eds) Stratigraphy and sedimentary evolution of western India. Gyanodaya Prakashan, Nainital, pp 74–103

Brigaud B, Pucéat E, Pellenard P, Vincent B, Joachimski MM (2008) Climatic fluctuations and seasonality during the Late Jurassic (Oxfordian-Early Kimmeridgian) inferred from δ^{18}O of Paris Basin oyster shells. Earth Planet Sci Lett 273:58–67

Dera G, Brigaud B, Monna F, Laffont R, Pucéat E, Deconinck J-F, Pellenard P, Joachimski MM, Durlet C (2011) Climatic ups and downs in a disturbed Jurassic world. Geology 39:215–218

Desai BG, Patel SJ (2009) Upper Callovian-Middle Oxfordian belemnite assemblage from Jara Dome, Western Kachchh. J Geol Soc India 74:343–356

Doyle P, MacDonald DIM (1993) Belemnite battlefields. Lethaia 25:65–80

Dromart G, Garcia J-P, Picard S, Atrops F, Lécuyer C, Sheppard SMF (2003a) Ice age at the Middle-Late Jurassic transition? Earth Planet Sci Lett 213:205–220

Dromart G, Garcia J-P, Gaumet F, Picard S, Rousseau M, Atrops F, Lecuyer C, Sheppard SMF (2003b) Perturbation of the carbon cycle at the Middle/Late Jurassic transition: geological and geochemical evidence. Am J Sci 303:667–707

Fürsich FT (1998) Environmental distribution of trace fossils in the Jurassic of Kachchh (western India). Facies 39:243–272

Fürsich FT, Oschmann W, Singh IB, Jaitly AK (1992) Hardgrounds, reworked concretion levels and condensed horizons in the Jurassic of western India: their significance for basin analysis. J Geol Soc Lond 149:313–331

Fürsich FT, Pandey DK, Callomon JH, Jaitly AK, Singh IB (2001) Marker beds in the Jurassic of the Kachchh Basin, western India: their depositional environment and sequence-stratigraphic significance. J Pal Soc India 46:173–198

Fürsich FT, Callomon JH, Pandey DK, Jaitly AK (2004a) Environments and faunal patterns in the Kachchh rift basin, western India, during the Jurassic. Riv Ital Pal Strat 110:181–190

Fürsich FT, Oschmann W, Pandey DK, Jaitly AK, Singh IB, Liu C (2004b) Palaeoecology of Middle to lower Upper Jurassic macrofaunas of the Kachchh Basin, western India: an overview. J Pal Soc India 49:1–26

Fürsich FT, Singh IB, Joachimski M, Krumm S, Schlirf M, Schlirf S (2005) Palaeoclimate reconstructions of the Middle Jurassic of Kachchh (western India): an integrated approach based on palaeoecological, oxygen isotopic, and clay mineralogical data. Palaeogeogr Palaeoclimatol Palaeoecol 217:289–309

Grant CW (1840) Memoir to illustrate a geological map of Cutch. Trans Geol Soc Lond Ser 2 5(2):289–326

Hallam A (2001) A review of the broad pattern of Jurassic sea-level changes and their possible causes in the light of current knowledge. Palaeogeogr Palaeoclimatol Palaeoecol 167:23–37

Jain S, Callomon JH, Pandey DK (1996) On the earliest known occurrence of the Middle Jurassic ammonite genus *Reineckeia* in the Upper Bathonian of Jumara, Kachchh, western India. Paläont Z 70:129–143

Jaitly AK, Singh CSP (1983) Discovery of the Late Bajocian *Leptosphinctes* Buckman (Jurassic Ammonitina) from Kachchh, western India. N Jb Geol Paläont Mh 2:91–96

Jenkyns HC (1996) Relative sea-level change and carbon isotopes: data from the upper Jurassic (Oxfordian) of central and southern Europe. Terra Nova 8:75–85

Kayal A, Bardhan S (1998) *Epistrenoceras* Bentz (Ammonoidea) from the Middle Jurassic of Kutch (western India): a new record and its chronostratigraphic implication. Can J Earth Sci 35:931–935

Krishna J, Westermann GEG (1987) The *Macrocephalites* associations (Jurassic ammonoidea) of Kachchh, western India. Can J Earth Sci 24:1570–1582

Krishna J, Pathak DB, Pandey B (1996a) Quantum refinement in the Kimmeridgian ammonoid chronology in Kachchh (India). GeoResearch Forum 1–2:195–204

Krishna J, Meléndez G, Pandey B, Pathak DB (1996b) Middle Oxfordian ammonites (Perisphinctinae) from Kachchh (India): biostratigraphic and palaeobiogeographic implications. Rev Esp Pal Num Extraord 140–147

Krishna J, Pathak DB, Pandey B (1998) Development of Oxfordian (Early Upper Jurassic) in the most proximally exposed part of the Kachchh Basin at Wagad outside the Kachchh Mainland. J Geol Soc India 52:513–522

Krishna J, Pathak DB, Pandey B, Ohja JR (2000) Transgressive sediment intervals in the Late Jurassic of Kachchh, India. GeoResearch Forum 6:321–332

Krishna J, Pandey B, Ojha JR (2009a) *Gregoryceras* in the Oxfordian of Kachchh (India): diverse eventful implications. Geobios 42:197–208

Krishna J, Pandey B, Pathak DB (2009b) Characterization of *Dichotomoceras* in the Oxfordian of Kachchh. J Geol Soc India 74:469–479

Krishna J, Pandey B, Ojha JR, Pathak DB (2009c) Reappraisal of the age framework, correlation, environment and nomenclature of Kachchh Mesozoic lithostratigraphic units in Wagad. J Sci Res Banares Hindu Univ Varanasi 53:1–20

Louis-Schmid B, Rais P, Bernasconi SM, Pellenard P, Collin P-Y, Weissert H (2007) Detailed record of the mid-Oxfordian (Late Jurassic) positive carbon-isotope excursion in two hemipelagic sections (France and Switzerland): a plate tectonic trigger? Palaeogeogr Palaeoclimatol Palaeoecol 248:459–472

Malchus N, Steuber T (2002) Stable isotope records (O, C) of Jurassic aragonitic shells from England and NW Poland: palaeoecologic and environmental implications. Geobios 35:29–39

McArthur JM, Janssen NMM, Reboulet S, Leng MJ, Thirlwall MF, van de Schootbrugge B (2007) Palaeotemperatures, polar ice-volume, and isotope stratigraphy (Mg/Ca, δ^{18}O, δ^{13}C, ^{87}Sr/^{86}Sr): the early cretaceous (Berriasian, Valanginian, Hauterivian). Palaeogeogr Palaeoclimatol Palaeoecol 248:391–430

Mutterlose J, Malkoc M, Schouten S, Sinninghe Damsté JS, Forster A (2010) TEX_{86} and stable δ^{18}O paleothermometry of early Cretaceous sediments: implications for belemnite ecology and paleotemperature proxy application. Earth Planet Sci Lett 298:286–298

Norris MS, Hallam A (1995) Facies variations across the Middle-Upper Jurassic boundary in Western Europe and the relationship to sea-level changes. Palaeogeogr Palaeoclimatol Palaeoecol 116:189–245

Pandey DK, Agrawal SK (1984) On two new species of the Middle Jurassic ammonite genus *Clydoniceras* Blake from Kachchh, western India. N Jb Geol Paläont Mh 6:321–326

Pandey DK, Callomon JH (1995) Contribution to the Jurassic of Kachchh, western India. III. The Middle Bathonian ammonite families Clydoniceratidae and Perisphinctidae from Pachchhham Island. Beringeria 16:125–145

Pandey DK, Westermann GEG (1988) First record of Bathonian *Bullatimorphites* (Jurassic Ammonitina) from Kachchh, India. J Paleontol 62:148–150

Pandey DK, Callomon JH, Fürsich FT (1994) On the occurrence of the Callovian ammonite *Parapatoceras tuberculatum* (Baugier & Sauze 1843) in Kachchh, western India. Paläontol Z 68:63–69

Pearce CR, Hesselbo SP, Coe AL (2005) The mid-Oxfordian (Late Jurassic) positive carbon-isotope excursion recognised from fossil wood in the British Isles. Palaeogeogr Palaeoclimatol Palaeoecol 221:343–357

Price GD, Sellwood BW (1997) "Warm" palaeotemperatures from high Late Jurassic palaeolatitudes (Falkland Plateau): ecological, environmental or diagenetic controls? Palaeogeogr Palaeoclimatol Palaeoecol 129:315–327

Rais P, Louis-Schmid B, Bernasconi SM, Weissert H (2007) Palaeoceanographic and palaeoclimatic reorganization around the Middle-Late Jurassic transition. Palaeogeogr Palaeoclimatol Palaeoecol 251:527–546

Riboulleau A, Baudin F, Daux V, Hantzpergue P, Renard M, Zakharov V (1998) Evolution de la paléotempérature des eaux de la plate-forme russe au cours du Jurassique supérieur. CR Acad Sci Ser IIa Sci Terre Planets 326:239–246

Riccardi AC (1991) Jurassic and Cretaceous marine connections between the Southeast Pacific and Tethys. Palaeogeogr Palaeoclimatol Palaeoecol 87:155–189

Sellwood BW, Valdes PJ (2006) Mesozoic climates: general circulation models and the rock record. Sediment Geol 190:269–287

Sellwood BW, Valdes PJ, Price GD (2000) Geological evaluation of multiple general circulation model simulations of Late Jurassic palaeoclimate. Palaeogeogr Palaeoclimatol Palaeoecol 156:147–160

Shackleton NJ, Kennett JP (1975) Paleotemperature history of the Cenozoic and the initiation of Antarctic glaciation: oxygen and carbon isotope analyses in DSDP sites 277, 279, and 289. Init Rep DSDP 29:743–755

Singh IB (1989) Dhosa Oolite—A transgressive condensation horizon of Oxfordian age in Kachchh, western India. J Geol Soc India 34:152–160

Singh CSP, Jaitly AK, Pandey DK (1982) First report of some Bajocian-Bathonian (Middle Jurassic) ammonoids and the age of oldest sediments from Kachchh, W. India. Newsl Strat 11:37–40

Singh CSP, Pandey DK, Jaitly AK (1983) Discovery of *Clydoniceras* Blake and *Gracilisphinctes* Buckman (Bathonian-Middle Jurassic ammonites) in Kachchh, western India. J Paleontol 57:821–824

Smith AG, Smith DG, Funnell BM (1994) Atlas of Mesozoic and Cenozoic coastlines. Cambridge University Press, Cambridge

Spath LF (1927–1933) Revision of the Jurassic cephalopod fauna of Kachh (Cutch). Parts I-VI. Mem Geol Surv India Pal Ind New Ser 9(2):1–945

Tan FC, Hudson JD, Keith ML (1970) Jurassic (Callovian) paleotemperatures from Scotland. Earth Planet Sci Lett 9:421–426

Taylor BE, Ward PD (1983) Stable isotopic studies of *Nautilus macromphalus* Sowerby (New Caledonia) and *Nautilus pompilius* L. (Fiji). Palaeogeogr Palaeoclimatol Palaeoecol 41:1–16

Urey HC, Lowenstam HA, Epstein S, McKinney CR (1951) Measurement of paleotemperatures and temperatures of the Upper Cretaceous of England, Denmark, and the southeastern United States. Geol Soc Am Bull 62:399–416

Valdes P (1993) Atmospheric general circulation models of the Jurassic. Philos Trans R Soc Lond Ser B 341:317–326

Valdes PJ, Sellwood BW (1992) A palaeoclimate model for the Kimmeridgian. Palaeogeogr Palaeoclimatol Palaeoecol 95:47–72

Veizer J, Ala D, Azmy K, Bruckschen P, Buhl D, Bruhn F, Carden GAF, Diener A, Ebneth S, Godderis Y, Jasper T, Korte C, Pawellek F, Podlaha OG, Strauss H (1999) $^{87}Sr/^{86}Sr$, $\delta^{13}C$ and $\delta^{18}O$ evolution of Phanerozoic seawater. Chem Geol 161:59–88

Waagen W (1873–1875) Jurassic fauna of Kutch. The Cephalopoda. Mem Geol Surv India Pal Ind New Ser 9 1(1–4):1–247

Weissert H, Mohr H (1996) Late Jurassic climate and its impact on carbon cycling. Palaeogeogr Palaeoclimatol Palaeoecol 122: 27–43

Wierzbowski H (2002) Detailed oxygen and carbon isotope stratigraphy of the Oxfordian in Central Poland. Int J Earth Sci 91:304–314

Wierzbowski H (2004) Carbon and oxygen isotope composition of Oxfordian-Early Kimmeridgian belemnite rostra: palaeoenvironmental implications for Late Jurassic seas. Palaeogeogr Palaeoclimatol Palaeoecol 203:153–168

Wierzbowski H, Joachimski M (2007) Reconstruction of late Bajocian-Bathonian marine palaeoenvironments using carbon and oxygen isotope ratios of calcareous fossils from the Polish Jura Chain (central Poland). Palaeogeogr Palaeoclimatol Palaeoecol 254:523–540

Wierzbowski H, Joachimski M (2009) Stable isotopes, elemental distribution, and growth rings of belemnopsid belemnite rostra: proxies for belemnite life habitat. Palaios 24:377–386

Wierzbowski H, Dembicz K, Praszkier T (2009) Oxygen and carbon isotope composition of Callovian-Lower Oxfordian (Middle-Upper Jurassic) belemnite rostra from central Poland: a record of a Late Callovian global sea-level rise? Palaeogeogr Palaeoclimatol Palaeoecol 283:182–194

Wynne AB (1872) Memoir on the Geology of Kutch. Mem Geol Surv India 9:1–293